Fisheries and Oceans Canada | Pêches et Océans Canada
Ecosystems and Oceans Science | Sciences des écosystèmes et des océans

Canadian Science Advisory Secretariat
Pacific Region **Science Response 2022/007**

GLASS SPONGE REEF ADAPTIVE MANAGEMENT ZONES FOR THE HECATE STRAIT AND QUEEN CHARLOTTE SOUND MARINE PROTECTED AREA, BRITISH COLUMBIA

Context

Marine Protected Areas (MPAs) play important roles in conserving marine ecosystems worldwide. Under Canada's *Ocean's Act*, Fisheries and Oceans Canada (DFO) established nine Glass Sponge Reef Marine Refuges in the Strait of Georgia and eight in Howe Sound, British Columbia. Further to that, DFO established the Hecate Strait and Queen Charlotte Sound (HSQCS) MPA (Figure 1) to protect glass sponge habitats within three spatially-distinct reef complexes—the Northern Reef, the Central Reefs, and the Southern Reef (Government of Canada 2017). Each reef complex is made up of three management zone types: the core protection zone (CPZ), adaptive management zone (AMZ) and vertical adaptive management zone (VMZ). While all harmful human activities are prohibited in the CPZs, the MPA Regulations allow for some limited fishing activities in the AMZs and VMZs—including recreational fisheries and Indigenous fishing for Food, Social and Ceremonial purposes. Currently, all commercial bottom-contact fishing and midwater trawling in the MPA is prohibited by *Fisheries Act* Variation Orders. While the HSQCS MPA is designed to protect unique marine ecosystems formed by glass sponge reefs, the effectiveness of the MPA depends on how well the AMZ boundaries function as a protective measure. The existing AMZ boundaries within the HSQCS MPA range from 0.6 to 4.5 km from the CPZ boundaries. The glass sponge reefs off British Columbia are the habitat for many commercially important fish and are subject to fishing pressure such as bottom-contact trawl fishing. Bottom-contact trawl fishing can result in physical damage to habitat directly, and also negatively impact on glass sponge reefs indirectly by suspending a large amount of sediment, which can then be transported into the CPZ.

Glass sponges are highly efficient water filterers that constantly filter and pump in organic and inorganic particles. However, they can quickly arrest their pumping activities in response to the exposure to sediments. Multiple arrests may reduce energy uptake of glass sponges, which could negatively affect their health; while the long-term effects of repeated sediment exposure and arrests on their health and population remain to be a knowledge gap (Grant et al. 2019). Grant et al. (2018) found that in the Strait of Georgia, glass sponges cease pumping (arrested) at suspended sediment concentration far lower than concentrations that can be triggered by bottom-contact trawling. Furthermore, Grant et al. (2019) found that different species of glass sponges in the HSQCS MPA respond differently to the exposure of suspended sediments. They showed that the distance required from the AMZs to the CPZs depends on ocean environmental conditions and suggested that the existing AMZs in the HSQCS MPA may not be adequate to achieve effective conservation.

DFO Oceans has requested DFO Science to: 1) assess whether the existing AMZ boundaries are sufficient to protect the glass sponge reefs from suspended sedimentation impacts of mobile, bottom contact fishing gear, and 2) estimate new AMZ boundaries if the current boundaries do not provide sufficient protection for the sponge reefs.

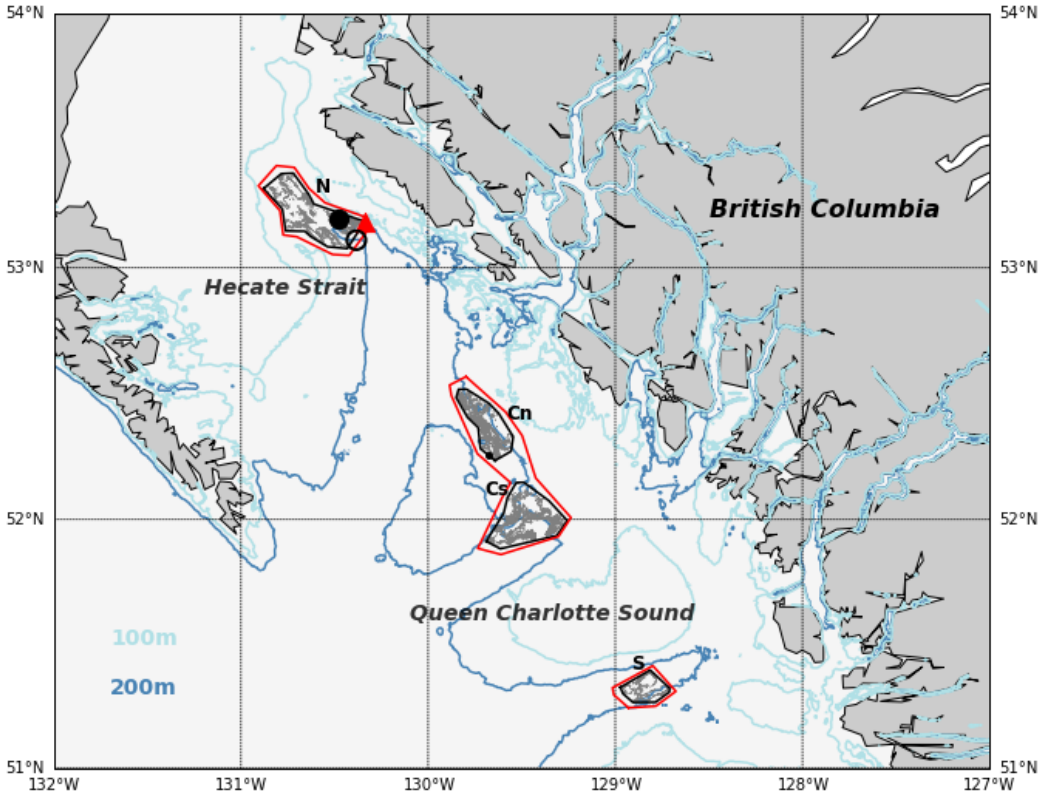

Figure 1. The HSQCS MPA located in British Columbia, Canada, consists of four glass sponge reefs (grey lines) enclosed by the core protection zones (black polygons) and adaptive management zones (red polygons). N, Cn, Cs, and S represent the northern, central northern, central southern and southern reefs respectively. The red triangle depicts a vertex of the core protection zone for the northern reef, where the model current is compared with observed currents at the two nearby sites (black open circle and black solid circle). The observed currents are from Grant et al. 2019 (black solid circle), and the Institute of Ocean Sciences (black open circle).

This Science Response Report results from the Regional Science Response Process of November 20, 2020 on Adaptive Management Zones for Hecate Strait/Queen Charlotte Sound Glass Sponge Reefs Marine Protected Areas.

Background

The existing AMZs in the HSQCS MPA were determined by considering potential exposure of suspended sediment transported by near-bottom currents to glass sponge reefs but without considering arresting threshold concentrations (Boutillier et al. 2013). Grant et al. (2018, 2019) conceptual work considered measured arresting threshold concentrations but without considering the direction of near-bottom currents. In this Science Response we use a sediment transport model forced by horizontally-variable near-bottom currents (Masson and Fine, 2012) and sponge reef arresting thresholds (Grant et al. 2019) to reassess the size and shape of the HSQCS MPA AMZs. According to Grant et al. (2019), *Rhabdocalyptus dawsoni* and *Heterochone calyx* arrested at sediment concentration of 2.8-6.4 mg/l and 5-10 mg/l respectively in the HSQCS MPA, while filtration rates from *Farrea occa* were too small to record. The background suspended sediment concentrations had a mean of 2.7 mg/l, with a standard deviation of 0.1 mg/l.

Sediment Modelling

This study uses a simple sediment transport model to estimate the sediment concentration distribution as a result of mobile, bottom-contact fishing gear. In our modelling, all particles are assumed to be spheres with no particle flocculation; particle resuspension is not considered; water turbulence or stratification is not considered. Observed sediment composition and size data are from Grant et al. (2019) and listed in Table 1.

Table 1. Representative grain size and composition for Hecate Strait. Information is derived from Grant et al. (2019). Note that there are slight differences between our composition percentage values and theirs because we use the sum of the component weights instead of the total weight provided in Grant et al. (2019).

Classification	Grain size(um)	Composition by weight (%)
>Fine sand	>212	69.19
Fine sand	212-106	15.74
Very fine sand	106-63	5.35
Coarse silt	63-45	2.93
Medium silt	45-20	6.08
Fine silt	<20	0.72

Vertical Motion

In the vertical, the particle settling velocity is governed by the Stokes settling equation. The total settling time for a particle suspended at a given height above the seabed is calculated for each grain size (Table 2).

Table 2. Sediment settling velocity and suspension time for each grain size from Grant et al. (2019).

Classification	Settling velocity (cm/s)	Suspension time (h) for the initial height of 5 m
>Fine sand	2.607	0.05
Fine sand	1.470	0.09
Very fine sand	0.425	0.33
Coarse silt	0.184	0.75
Medium silt	0.067	2.08
Fine silt	0.025	5.50

The settling velocity depends on the grain size (Table 2). The settling velocity varies from 2.607 cm/s for the > fine sand to 0.025 cm/s for the fine silt. The suspension time depends on both the grain size and the initial suspension height above seabed. Here we consider a sediment cloud with the initial suspension height of 5 m above seabed. The use of 5 m as the initial suspension height is explained in the Analysis and Response section. The suspension time, which varies linearly with the initial suspension height, is provided for sediment with an initial height of 5 m above seabed (Table 2). The suspension time for an initial height of 5 m above seabed ranges from 0.05 h for the > fine sand to 5.5 h for the fine silt. For a given grain size, any sediment below 5 m settles prior to the sediment at 5 m.

Horizontal Motion

In the horizontal, sediment motion is forced by tidal and non-tidal currents. The particle dispersion is not considered. The horizontal travel distance and direction for the particle before settling on the seabed is calculated by multiplying 4-h averaged velocities by the settling time,

since the settling time for the sediment that could cause arresting of *R. dawsoni* (threshold of 2.8-6.4 mg/l) is about 4 h for the study area (see the Analysis and Response section for detail).

The horizontal ocean currents that are used in forcing sediment transport are derived from a three-dimensional ocean circulation model for the British Columbia coastal and shelf waters (Masson and Fine, 2012), based on the Regional Ocean Modeling System (ROMS). The model has a resolution of 3 km in the horizontal and 30 layers in the vertical. The model includes eight major tidal constituents and circulation due to atmospheric forcing, river runoff and large-scale oceanic forcing. We use hourly bottom-layer currents for each hour in the first half of 2007, provided by Dr. Isaac Fain. The bottom layer has horizontally varying thickness, nevertheless, the detail of which is unavailable for us to consider here.

The hourly model bottom currents are shown for a CPZ vertex location (triangle, Figure 1) in the northern reef (Figure 2 and Figure 3). The temporal variations in the model currents are dominated by semidiurnal tidal currents, with spring-neap fluctuations (Figure 2). The model currents show a dominant flow direction, in the northwest-southeast direction (Figure 3). Strong currents, including the maximum current, occur roughly in the major flow direction.

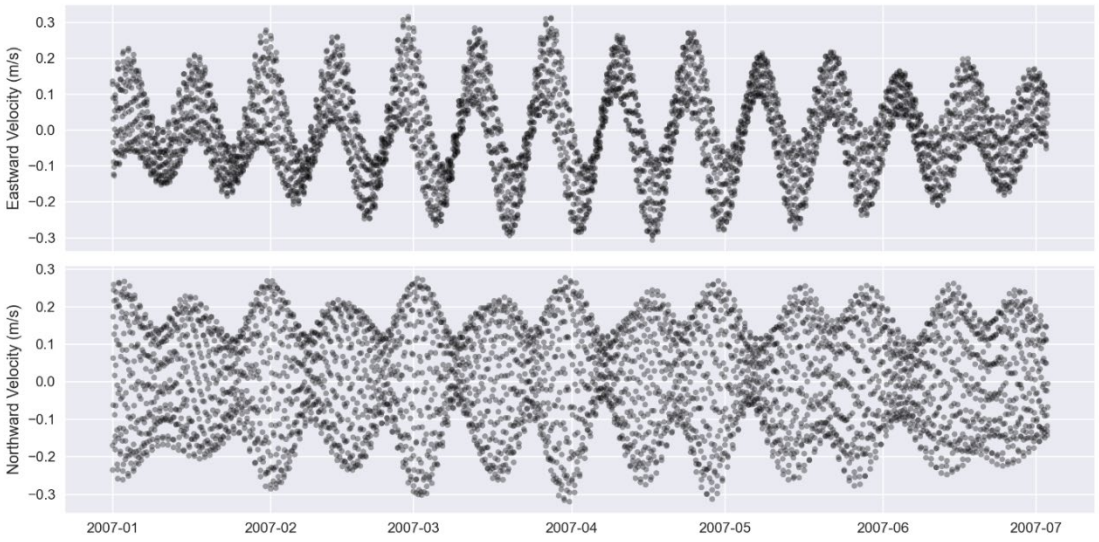

Figure 2. Time series of the hourly eastward and northward bottom currents at a CPZ vertex (triangle, Figure 1) of the northern reef. The currents are from Masson and Fain (2012).

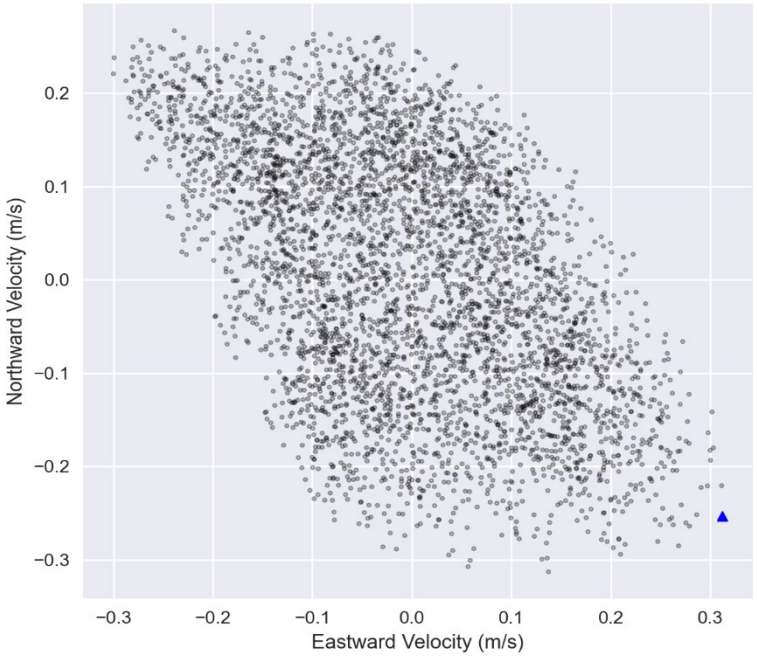

Figure 3. The scatter plot of the hourly model bottom currents at a CPZ vertex (triangle, Figure 1) of the northern reef for half a year. The maximum hourly current is depicted by the blue triangle.

Next we compare the model bottom currents with observed currents. Grant et al. (2019) collected near-bottom current data at a site (solid circle, Figure 1) near the above vertex location for a period of shorter than a month. Their observed currents averaged over 4 hours during flood cycles were 0.274 and 0.120 m/s at 5 and 1 m above seabed, respectively. The maximum model bottom current averaged over 4 hours at the nearby CPZ vertex (triangle, Figure 1) is 0.368 m/s during the first half of 2007. For the maximum 4-h model current to be greater than the observed 4-h current is expected because the latter is based on a data record shorter than a month (Grant et al. 2019) and does not capture a complete spring-neap tidal cycle or as many storm events in half a year. Therefore, it is reasonable to assume that the model bottom currents can approximately represent the currents experienced by suspended sediments at about 5 m above seabed.

There are also moored current meter data at about 7 m above seabed at a nearby site (open circle, Figure 1) in the northern reef from July 2017 to June 2018. The time series data for 2018 show semi-diurnal tidal variations, with spring-neap tidal fluctuations (Figure 4). The scatter plot shows a dominant east-west flow direction, but the maximum current is almost perpendicular to the dominant direction (Figure 5). Strong currents can occur in any direction. The data for the second half of 2017 (not shown) have overall consistent flow patterns with those in the first half of 2018, which justifies the present use of half a year of model currents. The observed maximum 4-h current is 0.367 m/s for the first half of 2018, with the dominant flow direction in the east-west direction. The maximum 4-h model current magnitude at the nearby CPZ vertex (triangle, Figure 1) is 0.368 m/s for the first half of 2007, with the dominant direction in the northwest-southeast direction. In addition, there is a high degree of temporal variability in the observed currents not seen in the modelled currents. It is important to keep in mind that there is good model-observation agreement in the magnitude of the maximum current and there is large model-observation discrepancy in the direction of strong currents, including the maximum current.

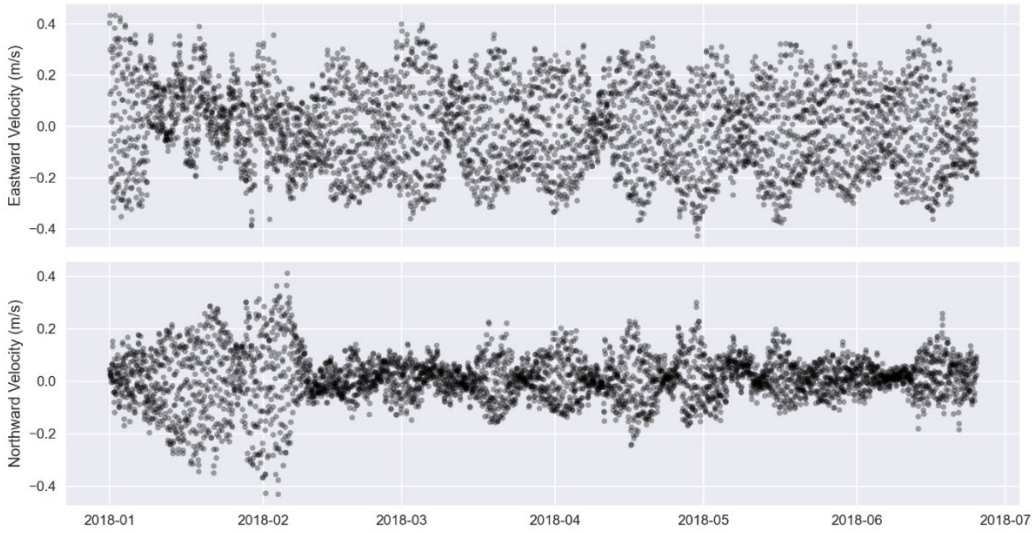

Figure 4. Time series of the hourly observed eastward and northward near-bottom currents at a site (130º23'W, 53º6.5'N, open circle, Figure 1) in the northern reef.

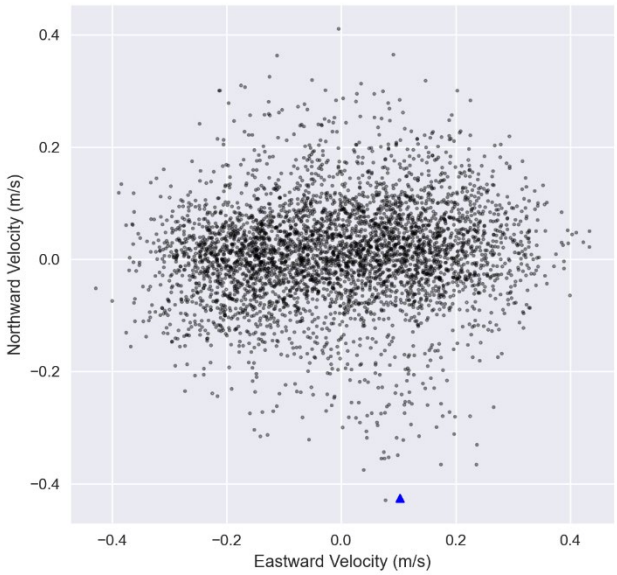

Figure 5. The scatter plot of the hourly observed near-bottom currents at a site in the northern reef (open circle, Figure 1) for half a year. The maximum hourly current is depicted by the blue triangle.

Analysis and Response

Impact Distance

The modelled sediment concentration distribution is compared with the known impact threshold concentrations of glass sponge reefs to estimate the potential impact distance of the sediment plume due to bottom-contact fishing every hour for half a year. We use a threshold concentration of 2.8 mg/l for *R. dawsoni* and of 5 mg/l for *H. calyx* in the HSQCS MPA respectively (Grant et al. 2019). These threshold concentrations are the lower ends of the arrest concentration ranges of 2.8-6.4 mg/l and 5-10 mg/l for *R. dawsoni and H. calyx*, respectively. The background sediment concentration of 2.7 mg/l is close to the lower ends of the observed

threshold concentrations and therefore is accounted for in order to protect the reefs from arresting. When the background concentration of 2.7 mg/l is accounted for, the effective threshold concentration for the fishing-induced sediment is 0.1 mg/l for *R. dawsoni* and of 2.3 mg/l for *H. calyx* in the HSQCS MPA respectively.

The initial concentration, grain size and suspension height of sediment, as well as ocean bottom currents determine the sediment travel distance and concentration distribution. The concentration distribution can be used to determine whether a species may be impacted by a sediment plume and to determine the impact distance.

Figure 6 shows the variation of the sediment height above seabed with the distance travelled for each grain size for an initial height of 5 m above seabed and a typical current speed of 0.35 m/s. It can be seen that the fine silt travels farthest (6.9 km) before settlement.

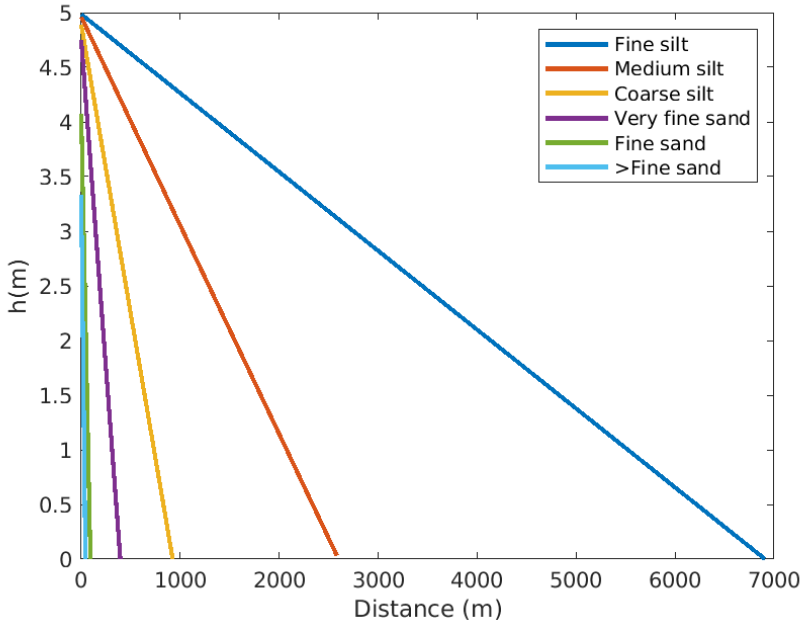

Figure 6. Distance each grain size found in the HSQCS MPA travels for an initial height of 5 m above seabed under a representative maximum 4-h current of 0.35 m/s.

Otter trawls, shrimp trawls, hook and line longlines, and prawn traps are commonly used fishing gears in the waters around the HSQCS MPA, with otter trawls and shrimp trawls causing much greater disturbance on bottom sediment than the other two (Boutillier et al. 2013). Otter trawls could generate suspended sediment concentrations as much as 200 mg/l within 2 m above seabed (Mengual et al. 2016). With some measures applied (e.g. jumper doors), suspended sediment concentrations could be reduced to as low as 20-100 mg/l; while the sediment can occasionally reach 6 m above seabed, at any time the sediment concentration at 4, 5 and 6 m is below 50%, 30% and 10% of the maximum concentration of about 200 mg/l, respectively (Mengual et al. 2016). Shrimp trawls could generate suspended sediment concentrations as much as 550 mg/l at 1-2 m above seabed, with the values decreased to 430 mg/l (about 80% of the maximum) at about 3 m above seabed (Schubel et al. 1978). As a precautionary measure, we use shrimp trawl as the proxy for mobile, bottom-contact fishing activities in this study. As such we use vertically variable initial sediment concentrations of 550, 550, and 430 mg/l at 1, 2, and 3 m above seabed, respectively. Nevertheless, there are no data for shrimp trawl above 3 m. Thus we further make use of the above percentage values relative to the maximum

concentration from otter trawl. The initial sediment concentrations used at 4 and 5 m above seabed are 110 (20% of 550) and 14 (2.5% of 550) mg/l respectively, with no sediment above 5 m.

Next we calculate the variations of the sediment concentration with distance travelled as follows, using the model bottom current (with an implicit assumption that the current variation with height can be neglected).

- Specify the initial concentration, which is partitioned across the particle size classes according to the sediment fractions in Table 1.
- Each fraction then settles at the rate determined by its settling velocity.
- A given size fraction is removed from the calculation once it settles to the bottom (see Table 2 for the time each size fraction with an initial height of 5 m is in the water column)
- Once a size class settles to the bottom it does not get re-suspended.

The variations of the sediment concentration with distance travelled are shown in Figure 7, for the initial concentrations of 550, 550, 430, 110, and 14 mg/l at 1, 2, 3, 4, and 5 m above seabed, respectively. The intersection point between the sediment concentration curve and the threshold line indicates the impact distance. It can be seen from Figure 7 that sediment at 4 m above seabed has the largest impact distance of 5.1 km to *R. dawsoni*, while sediment at 3 m above seabed has the largest impact distance of 2.3 km to *H. calyx*. Therefore, we will consider the impact of the sediment at 4 m only, using the effective threshold for *R. dawsoni*.

It should be noted that Figure 6 and 7 are similar to Figure 7c of Grant et al. (2019). It is unclear why their sedimentation concentration curve becomes zero without reaching the fine silt settlement distance.

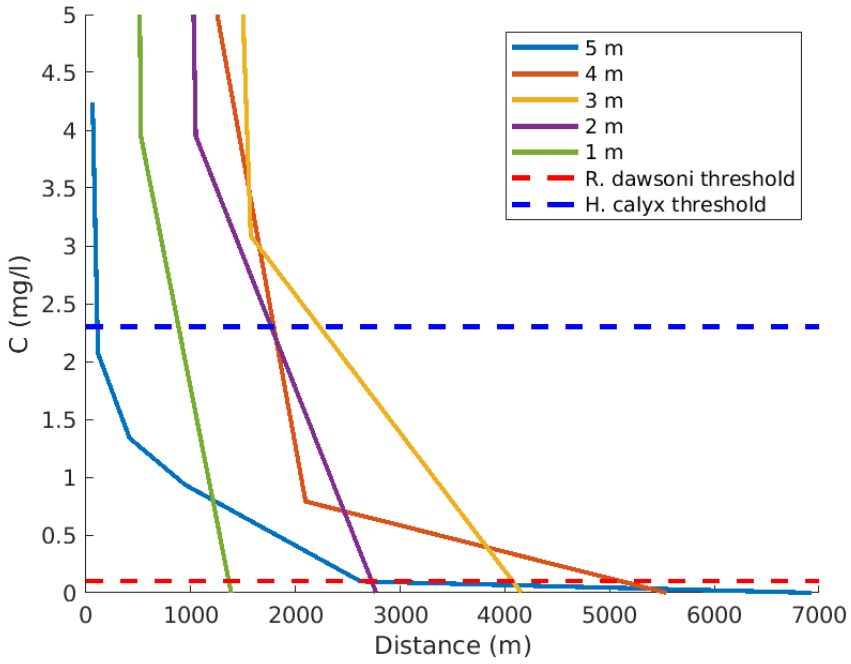

Figure 7. Change in concentration (C) of the sediment with distance under a representative maximum 4-h current of 0.35 m/s. Values are based on initial sediment concentrations of 550, 550, 430, 110 and 14 mg/l at 1, 2, 3, 4, and 5 m above seabed, respectively. The effective arrest threshold concentrations of R. dawsoni and H. calyx for the fishing-induced sediment are also shown (dashed line).

Approaches to Determine AMZs

Using a precautionary approach, we calculate the AMZ boundaries so that the sediment concentration in the CPZ would not exceed the arrest threshold of *R. dawsoni* (2.8 mg/l) when the background concentration of suspended sediment is accounted for. We chose *R. dawsoni* because it has the lowest observed arrest threshold among the three species of glass sponges in the HSQCS MPA.

Baseline approach

In the baseline approach we estimate the AMZ boundary by applying the maximum 4-h model currents during half a year to all directions, consistent with Grant et al. (2018, 2019) conceptual approach. The baseline approach is robust in the present application, because (1) the maximum 4-h model current magnitude agrees well with the maximum observed current magnitude and (2) the observed strong currents including the maximum current could be in any direction.

We calculate the vertices of the AMZ which ensures that the distance from the AMZ boundary to the CPZ boundary is not less than the maximum impact distance during half a year. For a typical CPZ, there are concave and convex vertices (Figure 8). For each concave CPZ vertex, we bisect the vertex angle outside the CPZ. The centre of a circle, which has a radii of one maximum impact distance and is tangential to the two segments that intersect at the CPZ vertex, is the corresponding vertex of the AMZ. For each convex CPZ vertex, we extend the two segments that intersect at the vertex. The centre of a circle, which has a radii of one maximum impact distance and is tangential to the two extension segments, is the corresponding vertex of the AMZ.

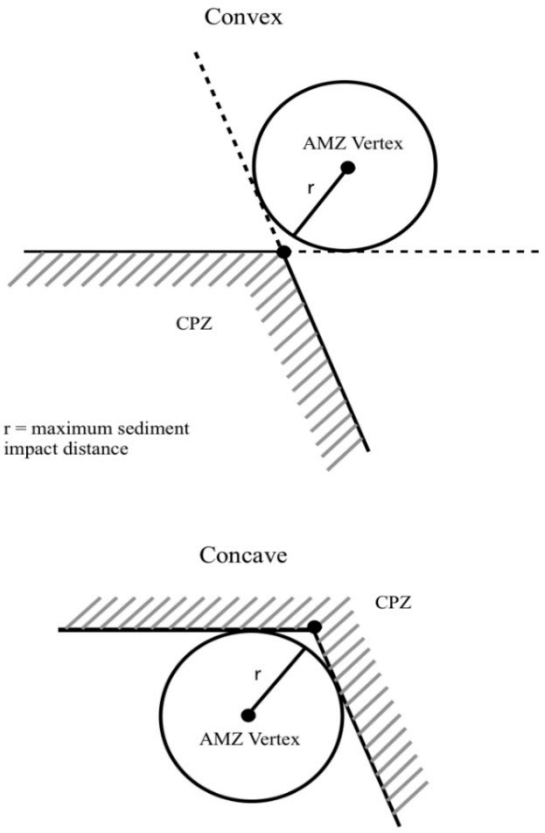

Figure 8. Schematic diagram on how to determine the AMZ vertex for the convex and concave CPZ vertices, respectively. At a convex vertex, the interior angle is smaller than 180º, while at a concave vertex, the interior angle is greater than 180º.

Alternative approach

As an alternative approach, we estimate the AMZ boundary by using both magnitude and direction of the 4-h model currents. As the current changes with time the impact distance and direction change for a given location, with a local impact area generally resembling an ellipse. In the alternative approach, we have developed an iterative search method to determine the AMZ boundary that accounts for both the current magnitude and direction. We choose minimum and maximum zonal coordinates at least one maximum impact distance from the most western and eastern CPZ vertices, respectively. For a given zonal coordinate, we first choose an appropriate starting location; proceed northward every 100 m until no ellipse points inside the CPZ and record the last zonal and meridional coordinate; then proceed from the starting location southward every 100 m until no ellipse points inside the CPZ and record the last zonal and meridional coordinate. Afterwards, we change the zonal coordinate by 100 m and repeat the above northward and southward search. Finally, we generate the alternative AMZ boundary that tightly encloses the area formed by the points with the recorded zonal and meridional coordinates and has the same number of vertices as the CPZ. Since the AMZ boundary is on the order of 1000 m away from the CPZ boundary, the 100 m spatial resolution is considered sufficient.

Results

Maps are generated to show the proposed AMZs (baseline and alternative), along with the glass sponge reefs, CPZs and existing AMZs (Figure 9-11). The AMZ vertex coordinate values from the baseline approach are provided in Table 3-6. Note that the initial baseline AMZs for the central northern reef and for the central southern reef overlap to some degree and thus are merged into a single AMZ. From the baseline approach using the maximum current magnitude, the distance between the proposed baseline AMZ boundary and CPZ boundary varies spatially from 3.5 to 10.0 km, and overall larger than that between the existing AMZ boundary and CPZ boundary (Figure 9-11), resulting in the increase in the proposed baseline AMZ sizes (Table 6) by 556 (237%), 801 (140%), and 239 (239%) square kilometres for the northern, central and southern reefs, respectively. The proposed alternative AMZs from the alternative approach are also larger than the existing AMZs, but to a smaller (approximately one third) degree than the baseline AMZs are (Table 6). Both the existing AMZs and the proposed alternative AMZs are determined by considering both magnitude and direction of the model currents, however, are limited by the discrepancy in the model currents as discussed in the Background section. The use of the maximum current magnitude in the baseline approach accounts for approximately two thirds of the increase in the proposed baseline AMZ areas over the existing AMZ areas.

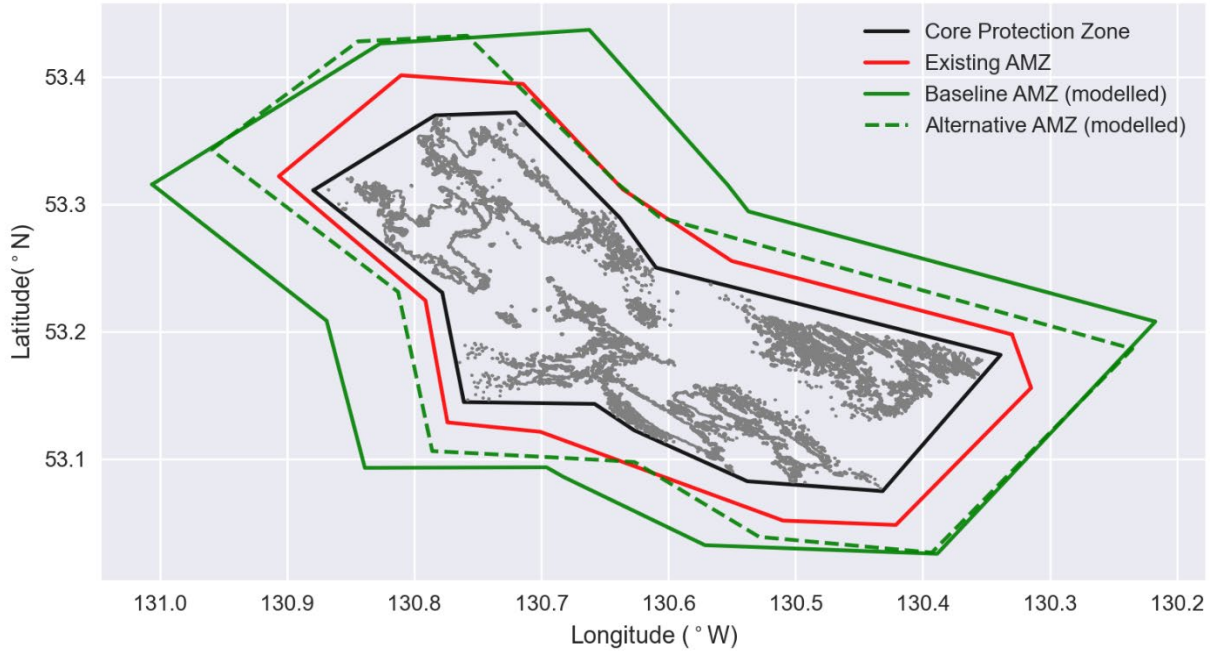

Figure 9. Map of the northern reef, CPZ, existing AMZ, new baseline AMZ, and new alternative AMZ.

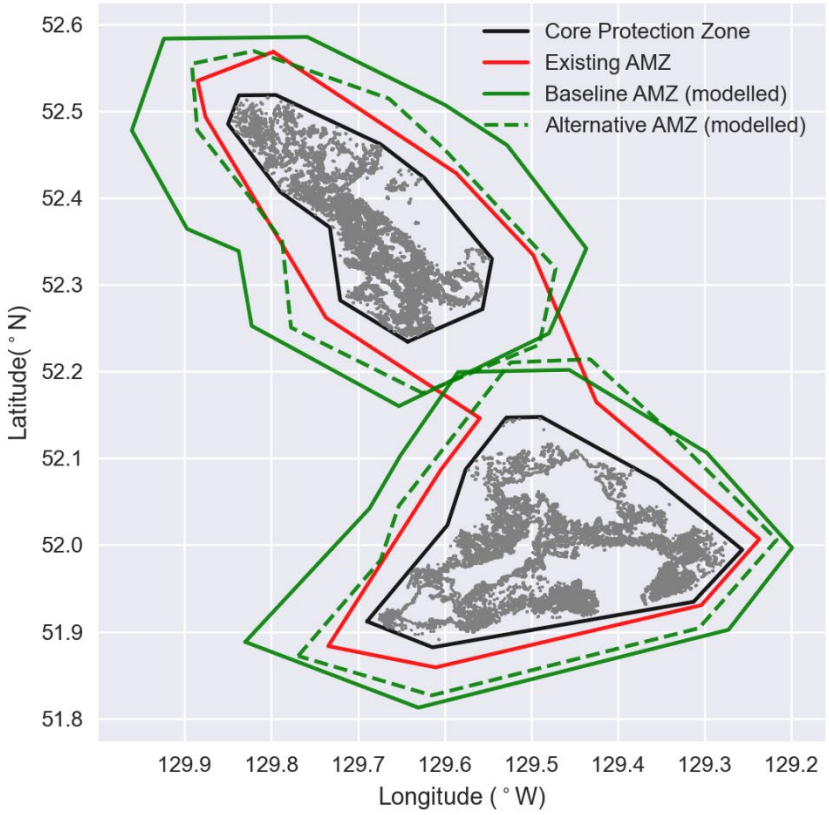

Figure 10. Map of the central reefs, CPZ, existing AMZ, new baseline AMZ, and new alternative AMZ.

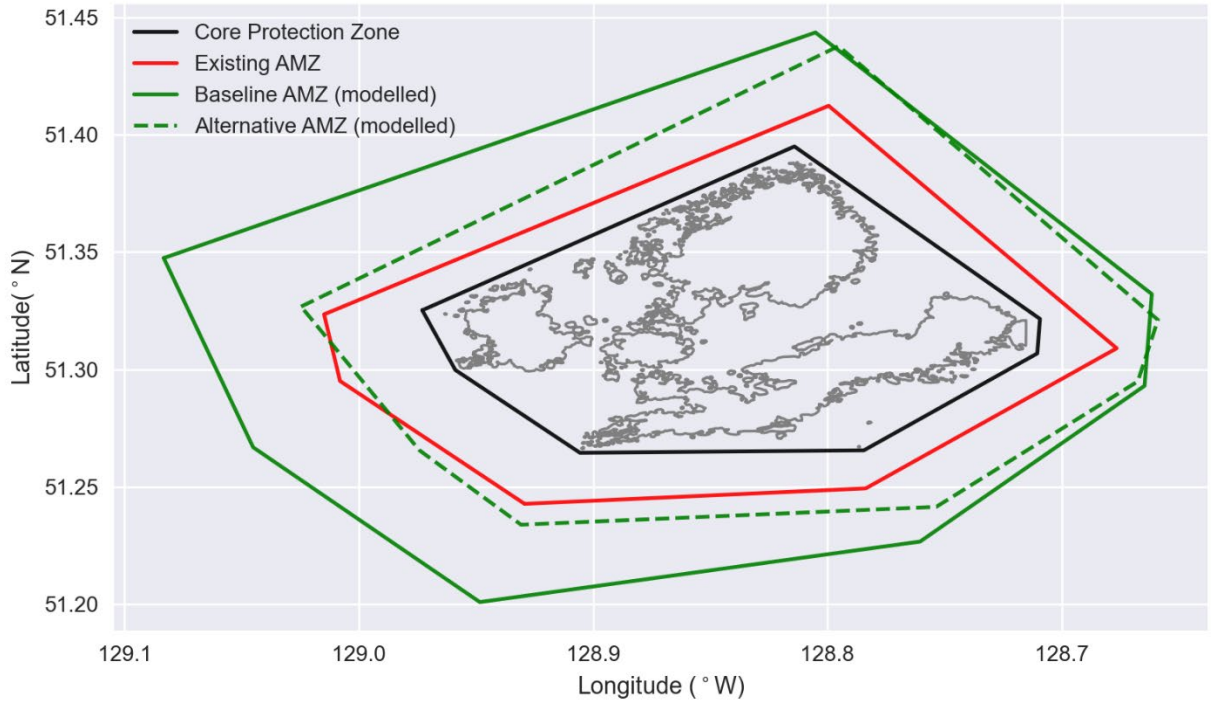

Figure 11. Map of the southern reef, CPZ, existing AMZ, new baseline AMZ, and new alternative AMZ.

Table 3. Coordinate values of the baseline AMZ for the northern reef.

Longitude (°W)	Latitude (°N)
131.00644	53.31583
130.82691	53.42638
130.66238	53.43717
130.55363	53.31561
130.5372	53.29462
130.21692	53.20815
130.38859	53.02586
130.57133	53.0326
130.68258	53.08614
130.69607	53.09376
130.83902	53.09331
130.86914	53.20883

Table 4. Coordinate values of the baseline AMZ for the central reefs.

Longitude (°W)	Latitude (°N)
129.65271	52.16006
129.82257	52.25254
129.8376	52.33876
129.89705	52.36426
129.96081	52.47772
129.92383	52.58343
129.75837	52.58537
129.59999	52.50728
129.5278	52.46061
129.4365	52.3417
129.47974	52.2438
129.57106	52.19959
129.45626	52.2018
129.29789	52.1066
129.19906	51.9969
129.27246	51.90239
129.63029	51.81265
129.83003	51.8884
129.68649	52.04236
129.65123	52.10272
129.59096	52.18996

Table 5. Coordinate values of the baseline AMZ for the southern reef.

Longitude (°W)	Latitude (°N)
129.08332	51.34744
128.80515	51.44351
128.66158	51.33209
128.66468	51.29304
128.76049	51.22669
128.94841	51.20092
129.04517	51.26684

Table 6. Comparison of CPZ and AMZ areas (square kilometres) for the northern (N), central northern (Cn), central southern (Cs), and southern (S) reefs.

Region	CPZ	Existing AMZ	Baseline AMZ	Alternative AMZ
N	524	235	791	468
Cn	313	573	1374	397
Cs	498			436
S	168	100	339	187

Discussion

Robustness of the baseline approach

To verify the robustness, we applied the baseline approach and the alternative approach using observed currents (see Figure 4 and 5) to determine AMZs for the northern reef only, by assuming that the near-bottom currents in the northern reef are horizontally invariable. This comparison between the baseline and alternative approaches is to determine if using flow direction information makes a difference or not. Figure 12 shows that the AMZs determined using the two approaches are close and within 10% of each other (841 square kilometres from the baseline approach and 762 square kilometers from the alternative approach). This is expected since large currents occur not only in the major flow direction but also in the minor flow direction. The baseline AMZ (791 square kilometres, Table 6) agrees within 10% with the above AMZs from the observed currents but the alternative AMZ (468 square kilometres, Table 6) is 39% smaller (Figure 12). As shown, the underestimation is in the southwest-northeast extent, clearly due to the model underestimation of the ocean currents in that direction (see Figure 3 and 5). This result indicates that the baseline approach is robust by applying the maximum model current to all directions, effectively mitigating the deficiency that the model does not reproduce large currents in the southwest-northeast direction. That being said, it is recognized that the verification is for the northern reef only.

In the alternative approach, the AMZ boundary is estimated by using both magnitude and direction of the 4-h model currents. Boutillier et al. (2013) tidal excursion approach also used both magnitude and direction of Masson and Fine's (2012) model currents in estimating the existing AMZs. So the alternative approach can also serve to demonstrate and explain why we do not recommend Boutillier et al. (2013) approach. As the current changes with time, the impact distance and direction change for a given location. During the 6 months of our simulations, the local impact area generally resembles an ellipse largely determined by the bottom tidal currents. For example, the approximate size and shape of the ellipse for the northern reef can be estimated by multiplying the model velocities in Figure 3 by the 2 hour integration time. However, the actual impact area should resemble a circle that can be estimated by multiplying the observed velocities in Figure 5 by 4 hour integration time. While the major (long) axis of the impact ellipse based on the model velocity is close to the diameter of the impact circle based on the observed velocity, the minor (short) axis of the impact ellipse is much shorter than the diameter of the impact circle. Therefore, both the alternative approach and Boutillier et al.(2013) approach substantially underestimate the local impact area. On the other hand, the baseline approach that uses the model maximum current magnitude results in an impact circle that well approximates the impact area based on the observed velocity.

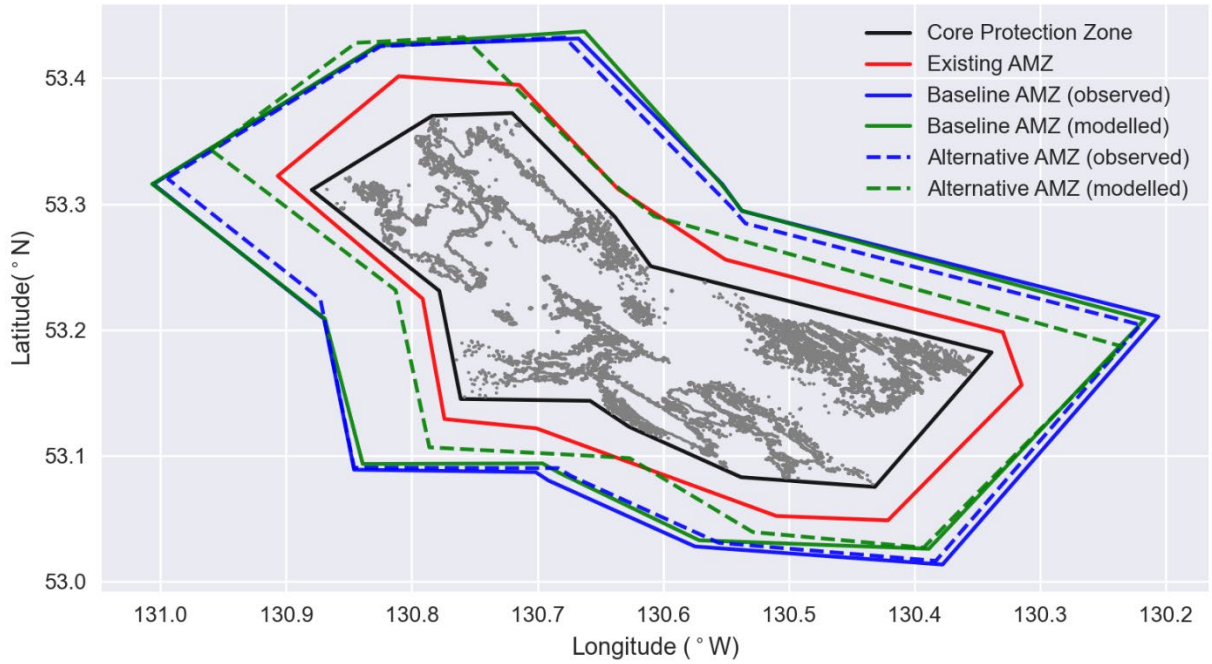

Figure 12. Map of the northern reef, CPZ, existing AMZ, and baseline AMZs using observed and modelled currents, as well as alternative AMZs using the observed and modelled currents.

Ways to reduce uncertainties and challenges to doing so

A number of assumptions are made on the ocean currents and sediment-related features that may introduce uncertainties in the results. Discrepancies between model and observed bottom currents are identified. Further work is recommended to reduce these uncertainties and discrepancies:

1. Improve circulation models to produce more accurate magnitude and direction of ocean currents, especially strong currents that can affect sediment transport most. The circulation models should sufficiently resolve the vertical structure of near-bottom currents, to allow use of different horizontal currents at different heights as sediment settles down, and the models could include the effects of the reefs on the near bottom currents in the models.
2. Collect more ocean current data in reef areas, for the validation of circulation models and for directly forcing sediment transport models if appropriate.
3. Observe bottom-contact fishing activity near the areas of interest to better quantify the range of disturbance heights and concentrations for different gear types, as well as horizontal extent. Know better the size distribution of the suspended sediment.
4. Use a more complex sediment transport model that takes into account more physical processes such as sediment dispersion and temporal changes in the natural suspended sediment concentration due to changes in the currents and waves.
5. Improve the knowledge of the arrest thresholds and on seasonal and spatial variations of the background sediment concentrations. Improve understanding of the impacts of arrests on health and population of glass sponges to guide how the arrest thresholds should be chosen and applied. Existing data on the physiology of glass sponges in British Columbia waters could be reanalyzed to revisit thresholds.

It is recognized that the sponges filter at low excurrent velocities, instruments to record filtering are specialized and approaches to positioning instruments are challenging. The biology of glass sponges is special and field work on them is extremely difficult due to their fragile nature and the deep-sea habitat. It is also challenging to think of ways in which the effect of sediment-induced arrests on populations of glass sponges could be determined in the field without causing extensive damage to a population of these sponges.

Conclusions

A sediment transport model forced by model bottom currents has been used to estimate proposed AMZs for the HSQCS MPA, in order to protect glass sponge reefs from the indirect effects of mobile, bottom-contact fishing gear. The proposed AMZ boundaries were calculated so that the glass sponge reefs were not subject to sediment concentrations in excess of the lowest observed pumping arrest threshold of *R. dawsoni*. The present study incorporates observed arrest thresholds from Grant et al. (2019), explicitly accounts for background sediment concentrations, and recognizes the fact that large currents can occur in any direction. The current study is therefore considered an advancement on Boutillier et al.'s (2013) work that determined the existing AMZs.

We have developed two approaches to determine the AMZ boundary. The baseline approach applies the maximum model current magnitude to all directions; while the alternative approach uses both magnitude and direction of the model currents. The baseline approach is considered robust because the maximum model current magnitude agrees well with the observed data, and the observed strong currents including the maximum current can be in any direction. It has also been shown that the alternative approach, and the approach used to estimate the existing AMZs, would underestimate impact areas because the modelled strong currents including the maximum current have large discrepancies in direction with the observed data.

A comparison of the proposed baseline AMZs with the existing AMZs shows considerable difference, with the proposed baseline AMZs larger than the existing AMZs. The increased area of the proposed baseline AMZs over the existing AMZs is due to the new results accounting for the observation in the northern sponge reef that the largest currents are not always in the direction of the dominant tidal flows, the introduction of the new arrest threshold and the background sediment in determining the AMZ boundary. Conservative (precautionary) options are adopted for some key model inputs (e.g. lowest observed arrest threshold and highest fishing impacts (shrimp trawl sediment profile)). The cumulative effects of using the conservative options have led to large AMZs. Resource managers can decide the level of precaution needed to provide adequate protection from potential sedimentation impacts of mobile, bottom-contact fishing activities. Further work may be considered according to the decided level of precaution.

Contributors

Contributor	Affiliation
Guoqi Han	DFO Science, Pacific Region
Jon Chamberlain	DFO Science, Pacific Region
Peter Chandler	DFO Science, Pacific Region
Di Wan	DFO Science, Pacific Region
Colin Webber	DFO Science, Pacific Region
Clayton Manning	DFO Oceans, Pacific Region, Client
Charles Hannah	DFO Science, Pacific Region, Reviewer
Sally Leys	University of Alberta, Reviewer

Approved by

Andrew Thomson
Regional Director
Science Branch, Pacific Region
Fisheries and Oceans Canada

December 14, 2021

Sources of Information

Boutillier, J., Masson, D., Fain, I., Conway, K., Lintern, G, O, M., Davies, S., Mahaux, P., Olsen, N., Nguyen, H. and Rutherford, K. 2013. The extent and nature of exposure to fishery induced remobilized sediment on the Hecate Strait and Queen Charlotte Sound glass sponge reef. DFO Can. Sci. Advis. Sec. Res. Doc. 2013/075. viii + 76 p.

Government of Canada. 2017. Hecate Strait and Queen Charlotte Sound Glass Sponge Reefs Marine Protected Areas Regulations SOR/2017-15.

Grant, N., Matveev, E., Kahn, A.S., and Leys, S.P. 2018. Suspended sediment causes feeding current arrests in situ in the glass sponge *Aphrocallistes vastus*. Mar Environ Res 137:111−120.

Grant, N., Matveev, E., Kahn, A.S., Archer, S.K., Dunham, A., Bannister, R.J., Eerkes-Medrano, D., and Leys, S.P. 2019. Effect of suspended sediments on the pumping rates of three species of glass sponge *in situ.* Marine Ecology Progress Series, 615, 79-100.

Masson, D., and Fine, I. 2012. Modeling seasonal to interannual ocean variability of coastal British Columbia. J. Geophysical Research - Oceans, 117, C10019, doi:10.1029/2012JC008151.

Mengual, B., Cayocca, F., Le Hir, P., Draye, R., Laffargue, P., Vincent, B., Garlan, T. 2016. Influence of bottom trawling on sediment resuspension in the 'Grande-Vasière' area (Bayof Biscay, France). Ocean Dyn 66: 1181−1207.

Schubel, J., Carter, H., Wilson, R., Wise, W., Heaton, M. 1978. Field investigations of the nature, degree, and extent of turbidity generated by open-water pipeline disposal operations. State University of New York at Stony Brook Marine Sciences Research Center. Dredged Material Research Program. Tech Rep D-78-30.

This Report is Available from the:

Centre for Science Advice (CSA)
Pacific Region
Fisheries and Oceans Canada
3190 Hammond Bay Road
Nanaimo, BC V9T 6N7

E-Mail: csap@dfo-mpo.gc.ca
Internet address: www.dfo-mpo.gc.ca/csas-sccs/

ISSN 1919-3769
ISBN 978-0-660-41858-2 Cat No. Fs70-7/2022-007E-PDF

Correct Citation for this Publication:

DFO. 2022. Glass Sponge Reef Adaptive Management Zones for the Hecate Strait and Queen Charlotte Sound Marine Protected Area, British Columbia. DFO Can. Sci. Advis. Sec. Sci. Resp. 2022/007.

Aussi disponible en français :

MPO. 2022. Zones de gestion adaptative des récifs d'éponges siliceuses pour la zone de protection marine du détroit d'Hécate et du bassin de la Reine-Charlotte en Colombie-Britannique. Secr. can. des avis sci. du MPO. Rép. des Sci. 2022/007.